Radiation-induced $1/f$ noise degradation of PNP bipolar junction transistors at different dose rates*

Qi-Feng Zhao(赵启凤)[1], Yi-Qi Zhuang(庄奕琪)[1], Jun-Lin Bao(包军林)[1,†], and Wei Hu(胡为)[2]

[1] School of Microelectronics, Xidian University, Xi'an 710071, China
[2] School of Mechano-Electronic Engineering, Xidian University, Xi'an 710071, China

(Received 28 June 2015; revised manuscript received 27 December 2015; published online 25 February 2016)

It is found that ionizing-radiation can lead to the base current and the $1/f$ noise degradations in PNP bipolar junction transistors. In this paper, it is suggested that the surface of the space charge region of the emitter-base junction is the main source of the base surface $1/f$ noise. A model is developed which identifies the parameters and describes their interactive contributions to the recombination current at the surface of the space charge region. Based on the theory of carrier number fluctuation and the model of surface recombination current, a $1/f$ noise model is developed. This model suggests that $1/f$ noise degradations are the result of the accumulation of oxide-trapped charges and interface states. Combining models of ELDRS, this model can explain the reason why the $1/f$ noise degradation is more severe at a low dose rate than at a high dose rate. The radiations were performed in a Co^{60} source up to a total dose of 700 Gy(Si). The low dose rate was 0.001 Gy(Si)/s and the high dose rate was 0.1 Gy(Si)/s. The model accords well with the experimental results.

Keywords: radiation, $1/f$ noise, bipolar junction transistors

PACS: 61.80.–x, 61.80.Ed, 85.40.Qx **DOI:** 10.1088/1674-1056/25/4/046104

1. Introduction

The PNP bipolar junction transistors are utilized in analog IC applications such as input stages, active loads, and current sources. Owing to surface effects, some types of PNP bipolar junction transistors are known to exhibit extreme sensitivities to ionizing radiation.[1] For many current bipolar linear technologies, the primary failure mechanism is the reduction of the current gain.[2–4] In 1991, it was found that bipolar junction transistors may exhibit the enhanced low dose rate sensitivity (ELDRS).[5] Since its initial report, all aspects concerning this effect (mechanism, modeling, testing, and recently studied ELDRS) has comprehensively been analyzed.[6–17] However, most of the radiation studies of Si bipolar junction transistors reported so far have mainly focused on experimental results about the radiation-induced changes in the measured electrical characteristics of the devices. To the authors' knowledge, very little data regarding $1/f$ noise performance degradation with the total dose and the dose rate have been reported for Si bipolar junction transistors.[18,19]

The total dose $1/f$ noise performances of PNP bipolar junction transistors radiated at different dose rates are presented. Based on the theory of carrier number fluctuation, a model is developed which identifies the physical mechanism responsible for the $1/f$ noise degradation. The model suggests that the $1/f$ noise degradations can be attributed to the accumulation of oxide-trapped charges and interface states. Combining models of ELDRS, the $1/f$ model can explain the reason why the $1/f$ noise degradation is more severe at a low dose rate than at a high dose rate. This work utilizes experiments and an analytical model to explain the mechanism responsible for radiation-induced $1/f$ noise degradation.

2. Model

2.1. Model of recombination current at the surface of the space charge region

When the base- emitter is under forward bias, the difference in quasi-Fermi energy level between electrons $\varepsilon_{\mathrm{Fn}}$ and holes $\varepsilon_{\mathrm{Fp}}$ is related to the voltage V_{EB} applied to the Base-Emitter junction, that is, $\varepsilon_{\mathrm{Fn}} - \varepsilon_{\mathrm{Fp}} = qV_{\mathrm{EB}}$,[20] where q is the electron charge. The carrier concentrations in the space charge region are given by

$$n(x) = n_{\mathrm{i}} \exp\left(\left(\varepsilon_{\mathrm{Fn}} - \varepsilon_{\mathrm{Fix}}\right)/(kT)\right), \tag{1}$$

$$p(x) = n_{\mathrm{i}} \exp\left(\left(\varepsilon_{\mathrm{Fix}} - \varepsilon_{\mathrm{Fp}}\right)/(kT)\right), \tag{2}$$

where $\varepsilon_{\mathrm{Fix}}$ is the intrinsic Fermi level in the space charge region, k is the Boltzmann constant, $T$is the absolute temperature, n_{i} is the intrinsic carrier concentration, $n(x)$ is the electron concentration, and $p(x)$ is the hole concentration.

The origin of the x axis is at the edge of the space charge region on the p side as shown in Fig. 1. In Fig. 1, E_{C} is the energy level of the Si conduction band bottom, E_{V} is the energy level of the Si value band top, and $\varepsilon_{\mathrm{Fi}}$ is the intrinsic Fermi level. At the origin of the x axis, the intrinsic Fermi level is $\varepsilon_{\mathrm{Fi0}}$ which we defined to be zero. From Fig. 1, it can be seen that the intrinsic Fermi level in the space charge region can be

*Project supported by the National Natural Science Foundation of China (Grant Nos. 61076101 and 61204092).
†Corresponding author. E-mail: baoing@126.com
© 2016 Chinese Physical Society and IOP Publishing Ltd

written approximately as[20]

$$\varepsilon_{\mathrm{Fix}} = -\frac{\varepsilon_{\mathrm{FiW}} - \varepsilon_{\mathrm{Fi0}}}{W}x = -q\frac{V_0 - V_{\mathrm{EB}}}{W}x, \quad (0 \le x \le W), \quad (3)$$

where W is the space charge region width; x is located in a range: $0 \le x \le W$; $V_0 = V_{\mathrm{Fn}} - V_{\mathrm{Fp}}$ is the built-in voltage, with $V_{\mathrm{Fn}} = kT\ln(N_{\mathrm{D}}/n_{\mathrm{i}})/q$ being the Fermi potential in the base, N_{D} the doping concentration at the base. $V_{\mathrm{Fp}} = kT\ln(n_{\mathrm{i}}/N_{\mathrm{A}})/q$ the Fermi potential in the emitter, and N_{A} the doping concentration at the emitter.

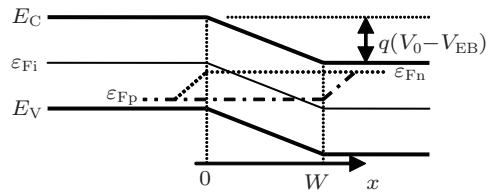


Fig. 1. Energy level of p–n junction under forward bias.

At $x = 0$, the hole concentration is given by

$$p_0 = n_{\mathrm{i}}\exp\left(\frac{-\varepsilon_{\mathrm{Fp}}}{kT}\right) = N_{\mathrm{A}} = n_{\mathrm{i}}\exp(-qV_{\mathrm{Fp}}/(kT)). \quad (4)$$

At $x = W$, the electron concentration is given by

$$\begin{aligned} n_W &= n_{\mathrm{i}}\exp\left(\frac{\varepsilon_{\mathrm{Fn}} - q(V_0 - V_{\mathrm{EB}})}{kT}\right) \\ &= N_{\mathrm{D}} = n_{\mathrm{i}}\exp(qV_{\mathrm{Fn}}/kT). \end{aligned} \quad (5)$$

From Eq. (4) we can obtain an expression for $\varepsilon_{\mathrm{Fp}}$:

$$\varepsilon_{\mathrm{Fp}} = qV_{\mathrm{Fp}}. \quad (6)$$

From Eq. (5) we can obtain an expression for $\varepsilon_{\mathrm{Fn}}$:

$$\varepsilon_{\mathrm{Fn}} = q(V_{\mathrm{EB}} - V_0 + V_{\mathrm{Fn}}) = q(V_{\mathrm{EB}} + V_{\mathrm{Fp}}). \quad (7)$$

In most analytical treatments of recombination in the space charge region, the spatial dependence is neglected;[4] instead, it is usually assumed that the total recombination rate can be obtained from the behavior of the peak recombination rate. However, in a radiated polar junction transistor, this assumption is subject to important limitations.[21] It is necessary to include the recombination current throughout the surface of the space charge region of the emitter-base junction to adequately describe the effects of radiation. The recombination current at the surface of the space charge region may be calculated by integrating the recombination rate over the surface of the emitter-base space charge region. It can be given by

$$I_{\mathrm{s}} = qL\int_0^W v_{\mathrm{th}}\sigma_{\mathrm{s}}N_{\mathrm{it}}\frac{n_{\mathrm{s}}p_{\mathrm{s}} - n_{\mathrm{i}}^2}{n_{\mathrm{s}} + p_{\mathrm{s}} + 2n_{\mathrm{i}}}\mathrm{d}x, \quad (8)$$

where L is the emitter perimeter, $s = v_{\mathrm{th}}\sigma_{\mathrm{s}}N_{\mathrm{it}}$ is the surface recombination velocity, N_{it} is the interface trap density, σ_{s} is the trap cross section, v_{th} is the electron thermal velocity, n_{s} is the surface electron concentration, and p_{s} is the surface hole concentration.

For a PNP bipolar junction transistor, an oxide-trapped charge causes the surface region of an n-type base to fall into accumulation. As the base is usually in accumulation mode, the following correlation between the surface potential V_{s} and oxide-trapped charge N_{ot} is valid:[22]

$$V_{\mathrm{s}} = \frac{kT}{q}\ln\left(\frac{N_{\mathrm{ot}}^2q^2}{2\varepsilon kTN_{\mathrm{A}}}\right). \quad (9)$$

We assume that the surface potential at the surface of the space charge region is approximately equal to the surface potential at the surface of the base. The surface potential would make the potential at the surface of the space charge region bend. At the same time, the accumulation of the base forces a reduction in the width of the space charge region at the surface as shown in Fig. 2. A reduced width of the space charge region can be given by

$$W = \sqrt{\frac{2\varepsilon(V_{\mathrm{D}} - V_{\mathrm{EB}} - V_{\mathrm{s}})}{qN_{\mathrm{D}}}}. \quad (10)$$

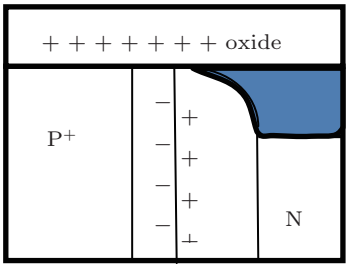


Fig. 2. (color online) Cross-section of the emitter base junction, illustrating accumulation regions in the presence of positive oxide charge.

The carrier concentrations at the surface of the space charge region can be given by

$$n_{\mathrm{s}} = n(x)\exp\left(\frac{qV_{\mathrm{s}}}{kT}\right), \quad (11)$$

$$p_{\mathrm{s}} = p(x)\exp\left(-\frac{qV_{\mathrm{s}}}{kT}\right). \quad (12)$$

Combining Eqs. (1), (3), (7), and (11), the surface recombination becomes

$$n_{\mathrm{s}} = n_{\mathrm{i}}\exp\left(\frac{q(V_{\mathrm{EB}} + V_{\mathrm{Fp}} + V_{\mathrm{s}})}{kT} + q\frac{V_0 - V_{\mathrm{EB}}}{W}x\right). \quad (13)$$

Combining Eqs. (2), (3), (6), and (12), the surface recombination becomes

$$p_{\mathrm{s}} = n_{\mathrm{i}}\exp\left(-q\frac{V_0 - V_{\mathrm{EB}}}{W}x - qV_{\mathrm{Fp}} - qV_{\mathrm{s}}\right). \quad (14)$$

The surface recombination can be expressed by

$$U(x) = v_{\mathrm{th}}\sigma_{\mathrm{s}}N_{\mathrm{it}}\frac{n_{\mathrm{s}}p_{\mathrm{s}} - n_{\mathrm{i}}^2}{n_{\mathrm{s}} + p_{\mathrm{s}} + 2n_{\mathrm{i}}}. \quad (15)$$

Combining Eqs. (13), (14), and (15), the surface recombination becomes

$$U(x)=\frac{1}{2}v_{\rm th}\sigma_{\rm s}N_{\rm it}n_{\rm i}\frac{\exp\left(\dfrac{qV_{\rm EB}}{kT}\right)-1}{\exp\left(\dfrac{qV_{\rm EB}}{2kT}\right)\cosh\left\{\dfrac{q}{kT}\left[\dfrac{x(V_0-V_{\rm EB})}{W}+V_{\rm EB}/2+V_{\rm Fp}+V_{\rm s}\right]\right\}+1}. \quad (16)$$

Assuming $V_{\rm BE}>4kT/q$, equation (16) is rewritten as

$$U(x)\approx\frac{1}{2}v_{\rm th}\sigma_{\rm s}N_{\rm it}n_{\rm i}\times\frac{\exp\left(\dfrac{qV_{\rm EB}}{2kT}\right)}{\cosh\left\{\dfrac{q}{kT}\left[\dfrac{x(V_0-V_{\rm BE})}{W}+V_{\rm EB}/2+V_{\rm Fp}+V_{\rm s}\right]\right\}}. \quad (17)$$

Substituting Eq. (17) into Eq. (8), equation (8) becomes

$$I_{\rm s}=\frac{1}{2}qLv_{\rm th}\sigma_{\rm s}N_{\rm it}n_{\rm i}\exp\left(\frac{qV_{\rm EB}}{2kT}\right)\left(\frac{kT}{q}\right)\left(\frac{W}{V_0-V_{\rm EB}}\right)\alpha, \quad (18)$$

where

$$\alpha=\tan^{-1}\left\{\exp\left[\frac{q}{kT}\left(\frac{x(V_0-V_{\rm EB})}{W}+V_{\rm EB}/2+V_{\rm Fp}+V_{\rm s}\right)\right]\right\}\Bigg|_0^W.$$

Equation (18) is the expression of the recombination current at the surface of the space charge region.

The opposing nature of oxide charge and interface traps may be verified with the aid of Fig. 3 which shows contour plots of the base surface recombination current $I_{\rm s}$ with surface recombination velocity and oxide charge as parameters on the y and x axes, respectively. As the surface recombination velocity is increased by one order of magnitude, the base surface recombination current increases approximately one order of magnitude. However, as oxide-trapped charge density is increased by one order of magnitude, the base current varies (reduces) much less than one order of magnitude. Therefore, the change in the surface recombination velocity will dominate the base surface recombination current response.

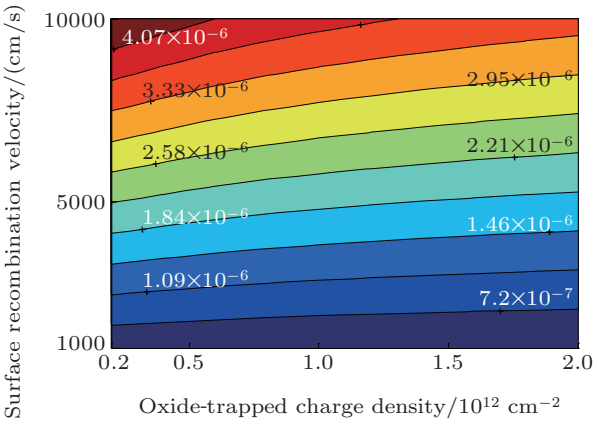


Fig. 3. (color online) Contour plots of base surface current response to an interactive combination of surface recombination velocity and oxide charge density.

2.2. Model of base surface $1/f$ noise

The low frequency $1/f$ noise in a bipolar junction transistor is currently explained by the fluctuations in carrier number[23–25] or Hooge Mobility.[26,27] It is generally admitted that the variation of power law exponent α of the current noise with the dc current provides the information about the noise type. When the exponent α is close to unity, the Hooge mobility fluctuations are believed to be responsible for the low frequency noise, while $\alpha\approx 2$ is indicative of carrier number fluctuations. Several $1/f$ noise models of a bipolar junction transistor were introduced in detail in Ref. [28]. For a bipolar junction transistor, the base current fluctuations are decomposed into surface and volume originated noise sources.[29] Often the surface $1/f$ noise component is the dominant component of the base $1/f$ noise.[30]

Experimentally, $1/f$ spectra have been observed in one or more tens of frequency ranges, requiring a process characterized by a time constant distributed over a wide range. Based on the theory of carrier number fluctuation,[31] there are two classes of carrier traps near the Si–SiO_2 interface, that is, oxide-trapped charges and interface states. The interface states exchange carriers with the conduction band or valence band of silicon as the generation-recombination centers due the SRH process, and, only a definite time constant is observed for interface states at a given energy. The oxide-trapped charge can exchange the carrier with the conduction band or valence band of silicon through the trap-tunneling process. The interface states are distinguished from the oxide-trapped charges by their location, thus by their shorter relaxation time constant than those of the oxide-trapped charges. Therefore the interface states contribute to relatively high frequency components of noise compared with the oxide-trapped charges whose time constants are longer than those of the interface states and have a wide range of time constants, which are necessary to generate a $1/f$ noise spectrum. So, the base surface $1/f$ noise of a PNP bipolar junction transistor may be ascribed to the low frequency fluctuations in the surface recombination current due to the dynamic trapping–detrapping of carriers into oxide-trapped charges.

The dynamic trapping–detrapping of carriers into oxide-trapped charges causes an oxide-trapped charge fluctuation $\delta N_{\rm ot}$, which should lead to a base surface current fluctuation $\delta I_{\rm s}$. According to Eq. (18), the fluctuation in the base surface recombination current is given by

$$\delta I_{\rm s}=\frac{\partial I_{\rm s}}{\partial\alpha}\frac{\partial\alpha}{\partial V_{\rm s}}\frac{\partial V_{\rm s}}{\partial N_{\rm ot}}\delta N_{\rm ot}+\frac{\partial I_{\rm s}}{\partial W}\frac{\partial W}{\partial V_{\rm s}}\frac{\partial V_{\rm s}}{\partial N_{\rm ot}}\delta N_{\rm ot}$$

$$= \left(\frac{\partial I_s}{\partial \alpha}\frac{\partial \alpha}{\partial V_s} + \frac{\partial I_s}{\partial W}\frac{\partial W}{\partial V_s}\right)\frac{\partial V_s}{\partial N_{ot}}\delta N_{ot}. \quad (19)$$

Combining Eqs. (9), (10), (18), and (19), equation (19) turns into

$$\delta I_s = I_s\left[\frac{C}{\alpha}\frac{q}{kT}\exp\left(\frac{qV_s}{kT}\right) - \frac{\varepsilon}{qN_D W^2}\right]\frac{kT}{q}\frac{2}{N_{ot}}\delta N_{ot}, \quad (20)$$

where

$$C = \frac{\exp\left[\frac{q}{kT}\left(\frac{V_{EB}}{2}+V_{Fp}\right)\right]}{1+\exp\left[\frac{2q}{kT}\left(V_{EB}/2+V_{Fp}+V_s\right)\right]} - \frac{\exp\left[\frac{q}{kT}\left(V_0-\frac{V_{EB}}{2}+V_{Fp}\right)\right]}{1+\exp\left[\frac{2q}{kT}\left(V_0-\frac{V_{EB}}{2}+V_{Fp}+V_s\right)\right]}.$$

According to Eq. (20), the $1/f$ noise power spectral density of the base current is given by

$$S_{IB} = S_{IBS} = I_s^2\left[\frac{C}{\alpha}\frac{q}{kT}\exp\left(\frac{qV_s}{kT}\right) - \frac{\varepsilon}{qN_D W^2}\right]^2 \times \left(\frac{kT}{q}\frac{2}{N_{ot}}\right)^2 S_{N_{ot}}, \quad (21)$$

where $S_{N_{ot}} = kT\lambda N_t(E)/(LWf)$[30] is the oxide-trapped charge spectral density, with $N_t(E)$ being the number of oxide-trapped charges per unit volume per unit energy (/eV/cm^3), and λ the attenuation tunneling distance; $N_{ot}(E) = \lambda N_t(E)$ is the number of oxide-trapped charges per unit area and per unit energy interval (/cm^2/eV), and $N_{ot}(E)$ is often continuously distributed in the forbidden gap. The N_{ot} can be obtained by integrating over the whole energy range

$$N_{ot} = \int_{E_V}^{E_C} N_{ot}(E)\,dE. \quad (22)$$

As the energy distribution of oxide-trapped charges is now not completely determined,[32] we make a simplified assumption that $N_{ot}(E)$ is uniformly distributed over the whole energy range, and expressed as

$$N_{ot}(E) = \frac{N_{ot}}{E_C - E_V}. \quad (23)$$

Then the correlation between $N_t(E)$ and N_{ot} can be obtained as follows:

$$N_{ot} = \lambda N_t(E)(E_C - E_V). \quad (24)$$

Combining Eqs. (21), (23), and (24), the $1/f$ noise power spectral density can be expressed as

$$S_{IBS} = I_s^2\left[\frac{C}{\alpha}\frac{q}{kT}\exp\left(\frac{qV_s}{kT}\right) - \frac{\varepsilon}{qN_D W^2}\right]^2 \times \frac{4(kT)^3}{LWq^2(E_C - E_V)N_{ot}}\frac{1}{f}. \quad (25)$$

Equation (25) shows that the accumulation of oxide-trapped charges N_{ot} and interface states N_{it} brings about changes in the base current noise.

3. Experiment and discussion

3.1. Experiment

The devices studied in this work were vertical PNP bipolar junction transistors obtained from a semiconductor manufacturer in China. Each device had an emitter with a doping surface of 1×10^{20} cm^{-3}, and the base doping is 1×10^{17} cm^{-3}. All transistors were irradiated with ionizing gamma-radiation from a Co^{60} source at room temperature. The low dose rate was 0.001 Gy(Si)/s and the high dose rate was 0.1 Gy(Si)/s. The parameters of the transistors were measured prior to and after 100, 300, 500, and 700 Gy(Si) of total dose exposure. The measured electrical parameters were the base current I_B and the collector current I_C, which were measured by an HP4156 Semiconductor Parameter Analyzer. The common emitter configuration circuit was used for noise measurements as shown in Fig. 4. Batteries were used to bias the base and collector terminals. The base load resistance $R_B \gg r_\pi$ was connected in series with the base (here $r_\pi = dV_{BE}/dI_B$ is the input base emitter resistance, I_B is the collector current). The noise signal S_{VC} from the collector load resistor R_C was amplified with a PARC113 low noise amplifier and then measured with an XD3020 noise measurement system which was described in Ref. [33]. In this high impedance model of operation, the base current noise S_{IB} makes the main contribution to the output noise S_{VC}, and is expressed as[34]

$$S_{IB} = \frac{S_{VC}}{\beta^2 R_C^2}, \quad (26)$$

where $\beta(\beta = I_C/I_B)$ is the current gain and I_C is the collector current.

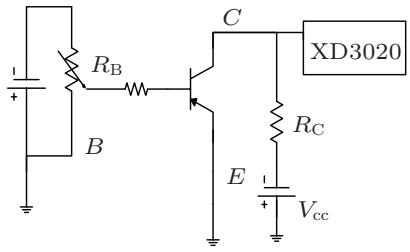


Fig. 4. Circuit used to bias the transistor for noise measurements.

3.2. Results and discussion

The relative change in the base current, $\Delta I/I_0$, is plotted versus total dose in Fig. 5. Figure 5 shows that $\Delta I/I_0$ increases with total dose increasing. The base current degradation mechanism can be explained as follows. With the accumulation of total dose, the oxide-trapped charges and the interface states increase. As recombination centers, the interface states cause the surface recombination rate to increase, which

makes the base surface recombination current increase. However, for a given surface recombination velocity, the oxide-trapped charges lead to a reduced recombination rate at the surface. The oxide-trapped charges accumulate in the surface of the base and force the holes to enter into the subsurface, which results in the decrease of recombination current. At the same time, the accumulation causes the width of the space charge region at the surface to decrease, which results in a lessening of the area for recombination current. As the surface recombination velocity is increased by one order of magnitude, the base surface recombination current increases approximately one order of magnitude. However, as oxide-trapped charge density is increased by one order of magnitude, the base current varies (decreases) much less than one order of magnitude. Therefore, the change in the surface recombination velocity will dominate the base surface recombination current response.

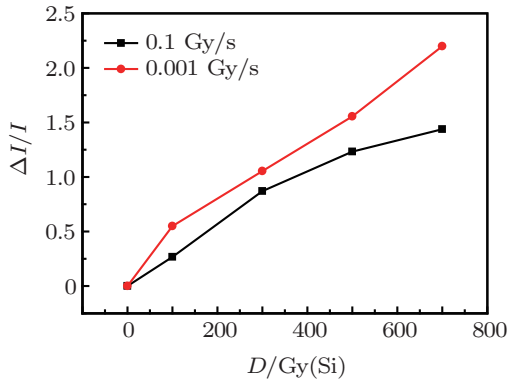


Fig. 5. (color online) Normalized base currents versus total dose.

Figures 6(a) and 6(b) show the base current noise spectra S_{IB} of the samples radiated at the dose rates of 0.1 Gy(Si)/s (Fig. 6(a)) and 0.001 Gy(Si)/s (Fig. 6(b)). Figure 6 shows that the low frequency noise performances are degraded significantly with accumulated total dose at the same rate for frequencies below 100 Hz.

The power spectral density of the base current is commonly expressed as follows:

$$S_{IB} = A + \frac{B}{f}, \tag{27}$$

where A is the amplitude of white noise (A^2/Hz) and B is the amplitude of $1/f$ noise (A^2/Hz). In Eq. (27), A and B may be extracted respectively from the measured noise spectrum by using the least-square fitting. In a frequency range of 10 Hz–100 Hz, the white noise is usually negligible.

From Eqs. (25) and (27), B can be obtained as

$$B = I_s^2 \left[\frac{C}{\alpha}\frac{q}{kT}\exp\left(\frac{qV_s}{kT}\right) - \frac{\varepsilon}{qN_D W^2}\right]^2 \times \frac{4(kT)^3}{LWq^2(E_C - E_V)N_{ot}}. \tag{28}$$

The amplitude of $1/f$ noise B is used to evaluate the base current noise degradation. The relative change of B can be written as

$$\frac{\Delta B}{B_0} = \frac{B - B_0}{B_0} = \frac{B}{B_0} - 1 = \frac{I_s^2}{I_{s0}^2}\frac{\left[\frac{C}{\alpha}\frac{q}{kT}\exp\left(\frac{qV_s}{kT}\right) - \frac{\varepsilon}{qN_D W^2}\right]^2}{\left[\frac{C_0}{\alpha_0}\frac{q}{kT}\exp\left(\frac{qV_{s0}}{kT}\right) - \frac{\varepsilon}{qN_D W_0^2}\right]^2} \times \frac{W_0}{W}\frac{N_{ot0}}{N_{ot}} - 1, \tag{29}$$

where B_0, N_{it0}, V_{s0}, W_0, N_{ot0}, C_0, and α_0 are the pre-radiation parameters, B, N_{it}, V_s, W, N_{ot}, C, and α are the post-radiation parameters.

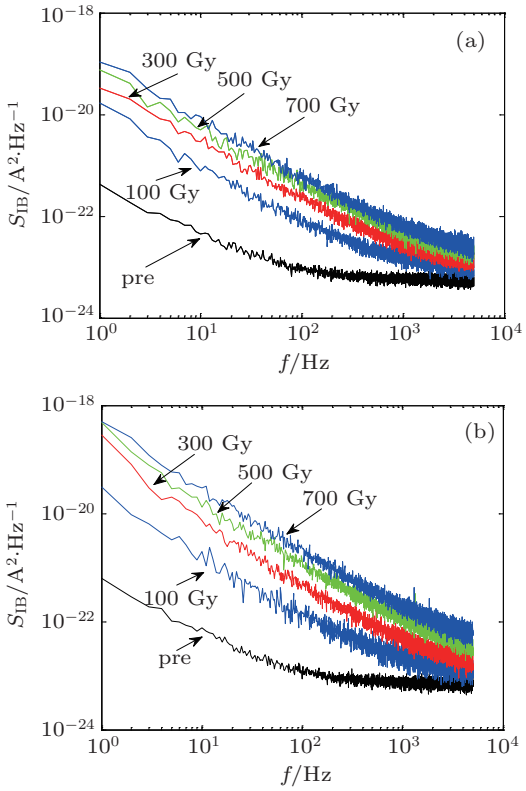


Fig. 6. (color online) Base current noise spectra versus total doses of (a) 0.1 Gy(Si)/s and (b) 0.01 Gy (Si)/s.

From Eq. (18), we can obtain

$$\frac{I_s^2}{I_{s0}^2} = \left(\frac{N_{it}}{N_{it0}}\frac{W}{W_0}\frac{\alpha}{\alpha_0}\right)^2. \tag{30}$$

Combining Eqs. (29) and (30) ,we can obtain

$$\frac{\Delta B}{B_0} = \left(\frac{N_{it}}{N_{it0}}\right)^2\left(\frac{\alpha}{\alpha_0}\right)^2\frac{W}{W_0}\frac{N_{ot0}}{N_{ot}} \times \frac{\left[\frac{C}{\alpha}\frac{q}{kT}\exp\left(\frac{qV_s}{kT}\right) - \frac{\varepsilon}{qN_D W^2}\right]^2}{\left[\frac{C_0}{\alpha_0}\frac{q}{kT}\exp\left(\frac{qV_{s0}}{kT}\right) - \frac{\varepsilon}{qN_D W_0^2}\right]^2} - 1. \tag{31}$$

The plots of relative change in the amplitude of $1/f$ noise, $\Delta B/B_0$, versus absorbed dose under radiations at two dose

rates are shown in Fig. 7. Figure 7 shows that $\Delta B/B_0$ increases with total dose increasing at the same rate, and at the same total dose level $\Delta B/B_0$ changes faster at the dose rate of 0.1 rad(Si)/s than at the dose rate of 10 rad(Si)/s.

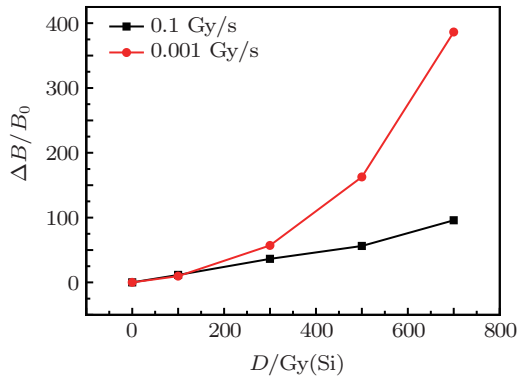


Fig. 7. (color online) Normalized amplitude of $1/f$ noise, $\Delta B/B_0$, versus total dose.

Let

$$\Gamma = \left(\frac{\alpha}{\alpha_0}\right)^2 \frac{N_{\rm ot0}}{N_{\rm ot}} \frac{W}{W_0} \frac{\left[\dfrac{C}{\alpha}\dfrac{q}{kT}\exp\left(\dfrac{qV_{\rm s}}{kT}\right) - \dfrac{\varepsilon}{qN_{\rm D}W^2}\right]^2}{\left[\dfrac{C_0}{\alpha_0}\dfrac{q}{kT}\exp\left(\dfrac{qV_{\rm s0}}{kT}\right) - \dfrac{\varepsilon}{qN_{\rm D}W_0^2}\right]^2}. \quad (32)$$

Figure 8 shows the plot of Γ versus oxide-trapped charge density based on Eq. (32). All analytical calculations are carried out by using MATLAB software. The following analytical calculation parameters are used: $T = 300$ K, $q = 1.6 \times 10^{-19}$ C, $\varepsilon_{\rm Si} = 8.85 \times 11.9 \times 10^{-14}$ F/cm, $V_{\rm EB} = 0.66$ V, $N_{\rm D} = 10^{17}$ cm^{-3}, $N_{\rm A} = 10^{20}$ cm^{-3}. It follows from Fig. 8 that Γ first increases and then increases as $N_{\rm ot}$ increases.

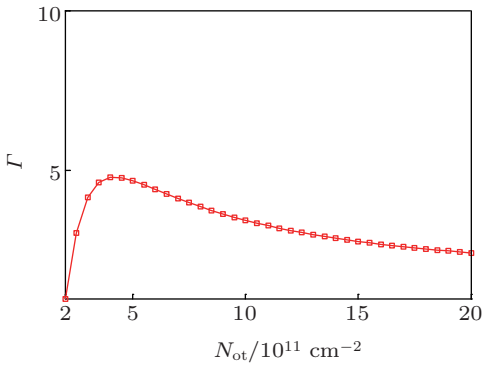


Fig. 8. (color online) Γ as a function of oxide-trapped charge density $N_{\rm ot}$.

The increase of base current noise spectrum $S_{\rm IB}$ with dose augment can be explained as follows. With the accumulation of total dose, the oxide-trapped charges and the interface states increase. Firstly, according to Eq. (25), the induced oxide-trapped charges and interface states can bring about an increase in base surface current, which makes the $1/f$ noise increase. Secondly, the induced oxide-trapped charges make more carriers participate in the dynamic trapping-detrapping. At the same time, the accumulation forces the width of the space charge region at the surface to decrease, which results in a smaller area at the surface of the space charge region. A smaller area can make the $1/f$ noise increase. The roles of the oxide-trapped charges are complex. According to Eqs. (31) and (32), the induced oxide-trapped charges can lead to an increase first and then a decrease. However, as oxide-trapped charge density is increased by one order of magnitude, the $\Delta B/B_0$ varies (decreases) much less than one order of magnitude. According to Eq. (31), $\Delta B/B_0$ is proportional to the interface state density. Combining the contributions made by the oxide-trapped charge and the interface state, we can draw a conclusion that the interface state dominates $1/f$ noise response. So, $1/f$ noise would increase with the dose augment.

Many models have been presented to explain ELDRS in a linear bipolar transistor. These models may be grouped into three main categories[35]: 1) space charge models,[36–40] 2) bimolecular process models,[41–46] and 3) a binary reaction rate model.[47] The phenomenon that at the same total dose level $\Delta I/I_0$ the $\Delta B/B_0$ changes faster at the dose rate of 0.001 Gy(Si)/s than at the dose rate of 0.1 Gy (Si)/s, can be explained with these models. According to these models, more interface states and oxide-trapped charges are induced at the low dose rate, which leads to more severe degradations of the base current and the base $1/f$ noise at the low dose rate.

4. Conclusions

In this paper, it is suggested that the surface of the space charge region of the emitter-base junction is the main source of the base surface $1/f$ noise for a PNP bipolar junction transistor with a heavily doped emitter. Based on the theory of carrier number fluctuation and the model of base surface recombination current, a $1/f$ noise model is developed, which can be used to explain the $1/f$ noise degradation induced by the radiation. Combining the models of ELDRS, this model can explain the fact that the $1/f$ noise is more severe at a low dose rate than at a high dose rate. The essential point of this work is to qualitatively describe the radiation-induced $1/f$ noise degradations of PNP bipolar transistors. Although many important aspects of the problem are neglected, the presented model may be helpful for understanding some of the features of bipolar radiation response.

References

[1] Witczak S C, Schrimpf R D, Galloway K F, Fleetwood D M, Schrimpf R D, Pease R L, Puhl J M, Schmidt D M, Combs W E and Suehle J S 1996 *IEEE Trans. Nucl. Sci.* **43** 3151
[2] Petrov A S and Ulimov V N 2012 *Microelectronics Reliability* **52** 2435
[3] Schrimpf R D 1996 *IEEE Trans. Nucl. Sci.* **43** 787
[4] Schmidt D M, Wu A, Schrimpf R D, Fleetwood D M and Pease R L 1996 *IEEE Trans. Nucl. Sci.* **43** 3032
[5] Enlow E W, Pease R L, Combs W E and Schrimpf R D 1991 *IEEE Trans. Nucl. Sci.* **38** 1342

[6] Pease R L, Schrimpf R D and Fleetwood D M 2009 *IEEE Trans. Nucl. Sci.* **56** 1894
[7] Fleetwood D M 2013 *IEEE Trans. Nucl. Sci.* **60** 1706
[8] Pease R L 2003 *IEEE Trans. Nucl. Sci.* **50** 539
[9] Rowsey N L, Law M E, Schrimpf R D, Fleetwood D M, Tuttle B R and Pantelides S T 2011 *IEEE Trans. Nucl. Sci.* **58** 2937
[10] Rashkeev S N, Cirba C R, Fleetwood D M, Schrimpf R D, Witczak S C, Michez A and Pantelides S T 2002 *IEEE Trans. Nucl. Sci.* **49** 2650
[11] Gonzalez-Velo Y, Boch J and Saigné F 2011 *IEEE Trans. Nucl. Sci.* **58** 2953
[12] Boch J, Saigné F, Schrimpf R D, Vaillé J R, Dusseau L and Lorf'evre E 2006 *IEEE Trans. Nucl. Sci.* **53** 3655
[13] Adell P C, Esqueda I S, Barbaby H J, Rax B and Johnston A J 2012 *IEEE Trans. Nucl. Sci.* **59** 3081
[14] Rowsey N L, Law M E, Schrimpf R D, Fleetwood D M, Tuttle B R and Pantelides S T 2012 *IEEE Trans. Nucl. Sci.* **59** 3069
[15] Xi S B, Lu W, Ren D Y, Zhou D, Wen L, Sun J and Wu X 2012 *Acta Phys. Sin.* **61** 236103 (in Chinese)
[16] Xi S B, Lu W, Wang Z K, Ren D Y, Zhou D, Wen L and Sun J 2012 *Acta Phys. Sin.* **61** 076101 (in Chinese)
[17] Ma W Y, Wang Z K, Lu W, Xi S B, Guo Q, He C F, Wang X, Liu M H and Jiang K 2014 *Acta Phys. Sin.* **63** 116101 (in Chinese)
[18] Prince J L and Stehlin R A 1971 *IEEE Trans. Nucl. Sci.* **18** 404
[19] Zhao Q F, Zhuang Y Q, Bao J L and Hu W 2015 *Acta Phys. Sin.* **64** 136104 (in Chinese)
[20] Sah C T, Noyce R N and Shockley W 1957 *Proc. IRE* **45** 1228
[21] Kosier S L, Schrimpf R D, Nowlin R N and Fleetwood D M 1993 *IEEE Trans. Nucl. Sci.* **40** 1276
[22] Pershenkov V S, Maslov V B, Cherepko S V, Shvetzov-Shilovsky I N, Belyakov V V, Sogoyan A V, Rusanovsky V I, Ulimov V N, Emelianov V V and Nasibullin V S 1997 *IEEE Trans. Nucl. Sci.* **44** 1840
[23] Stoisiek M and Wolf D 1980 *IEEE Trans. Electron. Dev.* **27** 1753
[24] Van der Ziel A, Zhang X and Pawlikiewicz A H 1986 *IEEE Trans. Electron. Dev.* **33** 1371
[25] Jäntsch O 1987 *IEEE Trans. Electron. Dev.* **34** 1100
[26] Kleinpenning T G M 1992 *IEEE Trans. Electron. Dev.* **39** 1501
[27] Kleinpenning T G M 1994 *IEEE Trans. Electron. Dev.* **41** 1981
[28] Deen M J and Pascal F 2004 *IEEE Proc.-Circuits Devices Syst.* **151** 125
[29] Mounib A, Ghibaudo G and Balestra F 1996 *J. Appl. Phys.* **79** 3330
[30] Zhuang Y Q and Sun Q 1993 *Noise and Its Minimizing Technology in Semiconductor Devices* (Beijing: National Defenses Industry Press) p. 83 (in Chinese)
[31] A L McWhorter A L 1957 *Semiconductor surface physics* (Philadelphia: University of Pennsylrnia Press)
[32] Zhuang Y Q and Sun Q 1991 *IEEE Trans. Electron Dev.* **38** 2540
[33] Bao J L, Zhuang Y Q and Du L 2004 *Chin. J. Sci. Instrum.* **25** 335 (in Chinese)
[34] Deen M J, Rumyantsev S L and Schroter M 1999 *J. Appl. Phys.* **85** 1192
[35] Pease R L, Schrimpf R D and Fleetwood D M 2009 *IEEE Trans. Nucl. Sci.* **56** 1894
[36] Fleetwood D M, Kosier S L, Nowlin R N, Schrimpf R D, Reber R A Jr, DeLaus M, Winokur P S, Wei A, Combs W E and Pease R L 1994 *IEEE Trans. Nucl. Sci.* **41** 1871
[37] Fleetwood D M, Riewe L C, Schwank J R, Witczak S C and Schrimpf R D 1996 *IEEE Trans. Nucl. Sci.* **43** 2537
[38] Witczak S C, Lacoe R C, Mayer D C, Fleetwood D M, Schrimpf R D and Galloway K F 1998 *IEEE Trans. Nucl. Sci.* **45** 2339
[39] Graves R J, Cirba C R, Schrimpf R D, Milanowski R J, Michez A, Fleetwood D M, Wiczak S C and Saigne F 1998 *IEEE Trans. Nucl. Sci.* **45** 2352
[40] Rashkeev S N, Cirba C R, Fleetwood D M, Schrimpf R D, Witczak S C, Michez A and Pantelides S T 2002 *IEEE Trans. Nucl. Sci.* **49** 2650
[41] Hjalmarson H P, Pease R L, Witczak S C, Shaneyfelt M R, Schwank J R, Edwards A H, Hembree C E and Mattsson T R 2003 *IEEE Trans. Nucl. Sci.* **50** 1901
[42] Tsetseris L, Schrimpf R D, Fleetwood D M, Pease R L and Pantelides S T 2005 *IEEE Trans. Nucl. Sci.* **52** 2265
[43] Boch J, Saigne F, Touboul A D, Ducret S, Carlotti J F, Bernard M, Schrimpf R D, Wrobel F and Sarrabayrouse G 2006 *Appl. Phys. Lett.* **88** 232113
[44] Boch J, Saigne F, Schrimpf R D, Vaille J R, Dusseau L and Lorfevre E 2006 *IEEE Trans. Nucl. Sci.* **53** 3655
[45] Fleetwood D M, Schrimpf R D, Pantelides S T, Pease R L and Dunham G W 2008 *IEEE Trans. Nucl. Sci.* **55** 2986
[46] Hjalmarson H P, Pease R L and Devine R 2008 *IEEE Trans. Nucl. Sci.* **55** 3009
[47] Freitag R K and Brown D B 1998 *IEEE Trans. Nucl. Sci.* **45** 2649